

PROPERTIES OF SHORT-WAVELENGTH OBLIQUE ALFVÉN AND SLOW WAVES

J. S. ZHAO^{1,2,3} Y. VOITENKO⁴ M. Y. YU^{5,6} J. Y. LU⁷ D. J. WU¹

¹ Purple Mountain Observatory, Chinese Academy of Sciences, Nanjing 210008, China; js_zhao@pmo.ac.cn

² Key Laboratory of Solar activity, National Astronomical Observatories, Chinese Academy of Sciences, Beijing 100012, China.

³ Key Laboratory of Modern Astronomy and Astrophysics, Nanjing University, Nanjing 210093, China.

⁴ Solar-Terrestrial Centre of Excellence, Space Physics Division, Belgian Institute for Space Aeronomy, Avenue Circulaire 3, B-1180 Brussels, Belgium

⁵ Institute for Fusion Theory and Simulation and Department of Physics, Zhejiang University, Hangzhou 310027, China

⁶ Institute for Theoretical Physics I, Ruhr University, D-44780 Bochum, Germany

⁷ College of Math and Statistics, Nanjing University of Information Science and Technology, Nanjing 210044, China. and Purple Mountain Observatory, Chinese Academy of Sciences, Nanjing, China

Submitted manuscript

ABSTRACT

Linear properties of kinetic Alfvén waves (KAWs) and kinetic slow waves (KSWs) are studied in the framework of two-fluid magnetohydrodynamics. We obtain the wave dispersion relations that are valid in a wide range of the wave frequency ω and plasma-to-magnetic pressure ratio β . The KAW frequency can reach and exceed the ion cyclotron frequency at ion kinetic scales, whereas the KSW frequency remains sub-cyclotron. At $\beta \sim 1$, the plasma and magnetic pressure perturbations of both modes are in anti-phase, so that there is nearly no total pressure perturbations. However, these modes exhibit also several opposite properties. At high β , the electric polarization ratios of KAWs and KSWs are opposite at the ion gyroradius scale, where KAWs are polarized in sense of electron gyration (right-hand polarized) and KSWs are left-hand polarized. The magnetic helicity $\sigma \sim 1$ for KAWs and $\sigma \sim -1$ for KSWs, and the ion Alfvén ratio $R_{Ai} \ll 1$ for KAWs and $R_{Ai} \gg 1$ for KSWs. We also found transition wavenumbers where KAWs change their polarization from left- to right-hand. These new properties can be used to discriminate KAWs and KSWs when interpreting kinetic-scale electromagnetic fluctuations observed in various solar-terrestrial plasmas. This concerns, in particular, identification of modes responsible for kinetic-scale pressure-balanced fluctuations and turbulence in the solar wind.

Subject headings: magnetohydrodynamics (MHD) – plasmas – solar wind – turbulence – waves

1. INTRODUCTION

Kinetic Alfvén waves (KAWs) have been receiving recently much attention in connection to understanding turbulence at kinetic scales in the solar wind and the near-Earth space environment (Chaston et al. 2008; Podesta 2013). KAWs can be generated by the MHD Alfvénic turbulence through an anisotropic cascade (Howes et al. 2008; Bian et al. 2010; Zhao et al. 2013), or through non-local coupling of the MHD Alfvén waves (Zhao et al. 2011; Zhao et al. 2014). These processes provide a pathway for the turbulence to dissipate via KAWs' damping (Schekochihin et al. 2009). KAWs have been found in many in situ spacecraft measurements (Chaston et al. 2008; Chaston et al. 2009; Huang et al. 2012; Podesta 2013). Identification of KAWs is usually accomplished by analyzing characteristic wave parameters, such as the ratio of electric to magnetic perturbations (Chaston et al. 2008; Chaston et al. 2009), magnetic compressibility (Podesta & TenBarge 2012), magnetic helicity (Howes et al. 2010; Podesta et al. 2011; He et al. 2012), or the profile of wave dispersion (Sahraoui et al. 2009; Sahraoui et al. 2010; Roberts et al. 2013).

On the other hand, kinetic slow waves (KSWs) have been found indirectly by analyzing the compressible turbulent fluctuations in the solar wind turbulence (Howes et al. 2012; Klein et al. 2012). KSWs have been

used in the interpretation of recent observations of small-scale pressure balanced structures (PBSs) in the solar wind (Yao et al. 2011; Yao et al. 2013), which exhibit an anti-correlation between the plasma and the magnetic pressure fluctuations. Since such small-scale PBSs can also be associated with KAWs, it is of great interest to investigate in more detail properties of the KAW and KSW modes at parallel and perpendicular kinetic scales, especially their differences.

Hollweg (1999) derived a two-fluid dispersion equation for KAWs and KSWs, and investigated properties of low-frequency KAWs, $\omega \ll \omega_{ci}$, where ω_{ci} is the ion cyclotron frequency. Another often made restricting assumption (see e.g. Shukla & Stenflo, 2000, and many others) was that the plasma beta $\beta \ll 1$ (β is the plasma/magnetic pressure ratio). These restrictions make problematic the applicability of obtained result to the solar wind, where β is often ~ 1 and the wave frequency ω that can approach and exceed ω_{ci} (Huang et al. 2012; Sahraoui et al. 2012). For the quasi-perpendicular Alfvén waves with frequencies reaching and extending above $\omega/\omega_{ci} = 1$, we will still use the same term KAW. The reason is that the wave dispersion and wave properties do not change much when the wave frequency crosses ω_{ci} .

In the present study we relax two above restrictions and study KAWs and KSWs in a wide range of wave and plasma parameters. A two-fluid plasma model is used to simplify derivations of the wave dispersion and

wave properties. The two-fluid plasma model has been proved to provide a good description for non-dissipative KAWs (Hollweg 1999; Bellan 2013). We suggest that the kinetic-scale PBSs observed in the solar wind can be interpreted not only in terms of KSWs, but also in terms of KAWs, and hence both these modes can contribute to PBSs. A more detailed analysis using new mode properties we obtained in this paper is needed to reveal the dominant mode in every particular event.

In Section 2, we derive the dispersion relation of the waves for the two-fluid model. Sections 3 and 4 discuss the properties of KAWs and KSWs, respectively. A discussion and conclusion is given in Section 5. The detailed derivation of the general dispersion equation is presented in Appendix A, the wave polarization and correlation properties are given in Appendix B, and Appendix C gives the analytic expressions of the linear wave dispersion relations and the linear responses in the low- β plasmas.

2. DISPERSION RELATION AND LINEAR RESPONSE

We shall start with the linear two-fluid equations

$$m_\alpha n_0 \partial_t \delta \mathbf{v}_\alpha = n_0 q_\alpha (\delta \mathbf{E} + \delta \mathbf{v}_\alpha \times \mathbf{B}_0) - \nabla P_\alpha, \quad (1)$$

$$\partial_t \delta n_\alpha = -\nabla \cdot (n_0 \delta \mathbf{v}_\alpha), \quad (2)$$

$$\nabla \times \delta \mathbf{B} = \mu_0 \delta \mathbf{J} + \frac{1}{c^2} \partial_t \delta \mathbf{E}, \quad (3)$$

$$\nabla \times \delta \mathbf{E} = -\partial_t \delta \mathbf{B}, \quad (4)$$

where the subscript $\alpha = i, e$ represents ions and electrons, respectively, m_α is the mass, q_α is the charge, $P_\alpha = T_\alpha n_\alpha$ is the thermal plasma pressure, T_α is the temperature, $\delta \mathbf{v}_\alpha$ is the perturbed velocity, $\mathbf{B}_0 = B_0 \hat{\mathbf{e}}_z$ is the uniform external magnetic field, $\delta \mathbf{J}$ is the perturbed current density, $\delta \mathbf{E}$ and $\delta \mathbf{B}$ are the electric and magnetic field perturbations, respectively, $n_\alpha = n_0 + \delta n_\alpha$, n_0 and δn_α are the background and perturbed number densities, respectively. We also assume $\omega_{pi}/\omega_{ci} \gg 1$, so that the displacement current in the Ampere's law (3) can be neglected.

We consider all perturbed variables δf in the form of plane waves, $\delta f \propto \delta f_k \mathbf{exp}(-i\omega t + i\mathbf{k} \cdot \mathbf{r})$, where ω is wave frequency and \mathbf{k} is the wave vector. The waves are further assumed to propagate in the (x, z) plane, that is, $\mathbf{k} = k_\perp \hat{\mathbf{e}}_x + k_z \hat{\mathbf{e}}_z$. The derivation of the general dispersion equation (A17) is given in Appendix A. Using corresponding approximations, the dispersion equation (A17) can be reduced to previously derived equations (Shukla & Stenflo 2000; Zhao et al. 2010; Chen & Wu 2011). Note that the two-fluid MHD plasma theory has several limitations as compared to the kinetic plasma theory. Most importantly, the two-fluid MHD cannot describe kinetic wave-particle interactions, like Landau damping, transit-time damping, and cyclotron damping. Also, some wave modes, like ion Bernstein mode, can only be found in the kinetic theory. As a result, the highly oblique fast wave transforms into the ion Bernstein mode at $\omega > \omega_{ci}$ in the kinetic theory, whereas in the fluid theory it continuously extends from $\omega < \omega_{ci}$ to the electron cyclotron frequency $\omega \rightarrow \omega_{ce}$ (Sahraoui et al. 2012). As far as the highly oblique KAWs are concerned, the wave properties given by the two-fluid MHD are consistent nearly with those given by the kinetic theory (Sahraoui et al. 2012;

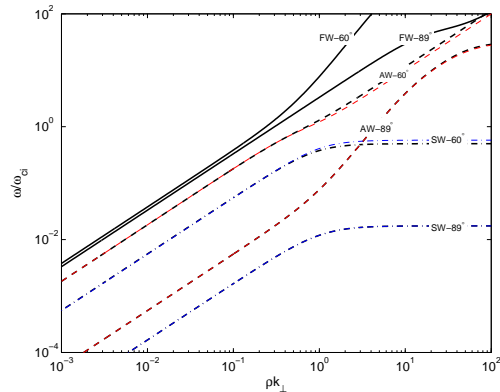


FIG. 1.— Comparison of the dispersion relations (6) (thin dashed lines are for Alfvén waves; thin dot-dashed lines are for slow waves) with the wave modes obtained from the general dispersion equation (A17) (thick solid lines are for fast waves; thick dashed lines are for Alfvén waves; thick dot-dashed lines are for slow waves). The two propagation angles are $\theta = 60^\circ$ and 89° , and $\beta = 0.1$.

Hunana et al. 2013). In particular, the KAW dispersion relation is nearly the same in two theories in the low-beta plasmas (Hunana et al. 2013). The frequency of the quasi-perpendicular slow mode also rises slowly as compared to the fast mode. Therefore, we focus on the quasi-perpendicular Alfvén and slow modes, but not the fast mode.

For quasi-perpendicular propagation, $k_\perp \gg k_z$, the cubic dispersion equation in ω^2 (Equation (A17)) can be reduced to the quadratic equation for $\omega^2 \ll k^2 (V_T^2 + V_A^2)$:

$$\omega^4 \left[1 + \lambda_e^2 k_\perp^2 + \lambda_i^2 k_z^2 + (1 + \lambda_e^2 k_\perp^2)^2 \beta \right] - \omega^2 (1 + 2\beta + \rho^2 k_\perp^2) V_A^2 k_z^2 + \beta V_A^4 k_z^4 = 0, \quad (5)$$

which describes the dispersion relation of the Alfvén and slow waves, $\omega^2 \sim V_A^2 k_z^2$ and $\omega^2 \sim V_T^2 k_z^2$. Here $\beta = V_T^2/V_A^2$. The terms of the order $Q = m_e/m_i$ or smaller are neglected in Eq. (5). The straightforward solutions to this equation are

$$\omega^2 = \frac{V_A^2 k_z^2 (1 + 2\beta + \rho^2 k_\perp^2)}{2 \left(1 + \lambda_e^2 k_\perp^2 + \lambda_i^2 k_z^2 + (1 + \lambda_e^2 k_\perp^2)^2 \beta \right)} \times \left[1 \pm \sqrt{1 - 4\beta \frac{1 + \lambda_e^2 k_\perp^2 + \lambda_i^2 k_z^2 + (1 + \lambda_e^2 k_\perp^2)^2 \beta}{(1 + 2\beta + \rho^2 k_\perp^2)^2}} \right] \quad (6)$$

where “+” stands for KAWs and “-” for KSWs. Dispersion relation derived by Hollweg (1999) is recovered from (6) in the low-frequency limit $\lambda_i^2 k_z^2 \ll 1$ (hence $\omega^2 \ll \omega_{ci}^2$), and $(1 + \lambda_e^2 k_\perp^2)(1 + \beta) \simeq 1 + \beta + \lambda_e^2 k_\perp^2$.

Figure 1 compares numerical solutions of the general dispersion equation (A17) and the dispersion relations (6) obtained for the quasi-perpendicular wave propagation. At such oblique propagation, the fast mode has significantly higher frequencies than the other two modes. The remaining KAW and KSW modes behave differently. Similarly to the fast mode, the KAW mode frequency increases monotonously with increasing wavenumber and exceeds the ω_{ci} at some wavelength close to the ion gyroradius. On the contrary, the KSW frequency slows down it increase above the ion gyroradius scale and never cross

$\omega = \omega_{ci}$. From this figure one can see that the quasi-perpendicular dispersion relations (6) are also valid down to $\theta \sim 60^\circ$.

The physical quantities associated with the KAW and KSW dispersion relations can be easily obtained from Equations (A1)–(A6) and (A11)–(A15):

$$\delta \mathbf{B} = -i \frac{\omega_{ci}}{\omega} \Upsilon_1 \delta B_y \hat{\mathbf{e}}_x + \delta B_y \hat{\mathbf{e}}_y + i \frac{k_\perp}{k_z} \frac{\omega_{ci}}{\omega} \Upsilon_1 \delta B_y \hat{\mathbf{e}}_z, \quad (7)$$

$$\begin{aligned} \delta \mathbf{E} = & \frac{\omega}{k_z} \left(1 + \lambda_e^2 k^2 + \Upsilon_2 \frac{\tilde{T}_e}{\tilde{T}_i} \right) \tilde{T}_i \delta B_y \hat{\mathbf{e}}_x + i \frac{\omega_{ci}}{k_z} \Upsilon_1 \delta B_y \hat{\mathbf{e}}_y \\ & + \frac{\omega}{k_\perp} \left(1 + \lambda_e^2 k^2 + \Upsilon_2 \frac{\tilde{T}_e}{\tilde{T}_i} - \frac{1}{\tilde{T}_i} \right) \tilde{T}_i \delta B_y \hat{\mathbf{e}}_z, \end{aligned} \quad (8)$$

$$\begin{aligned} \delta \mathbf{v}_i = & i \frac{\omega_{ci}}{k_z} \left(\Upsilon_2 - \frac{V_A^2 k_z^2}{\omega^2} \right) \frac{\delta B_y}{B_0} \hat{\mathbf{e}}_x - \frac{V_A^2 k_z}{\omega} \frac{\delta B_y}{B_0} \hat{\mathbf{e}}_y \\ & + i \frac{\omega_{ci}}{k_\perp} (\Upsilon_2 - 1) \frac{\delta B_y}{B_0} \hat{\mathbf{e}}_z, \end{aligned} \quad (9)$$

$$\begin{aligned} \delta \mathbf{v}_e = & i \frac{\omega_{ci}}{k_z} \left(\Upsilon_2 - \frac{V_A^2 k_z^2}{\omega^2} + \lambda_i^2 k_z^2 \right) \frac{\delta B_y}{B_0} \hat{\mathbf{e}}_x \\ & - \frac{\omega}{k_z} \left(1 + \lambda_e^2 k^2 - Q \frac{V_A^2 k_z^2}{\omega^2} \right) \frac{\delta B_y}{B_0} \hat{\mathbf{e}}_y \\ & + i \frac{\omega_{ci}}{k_\perp} (\Upsilon_2 - \lambda_i^2 k_\perp^2 - 1) \frac{\delta B_y}{B_0} \hat{\mathbf{e}}_z, \end{aligned} \quad (10)$$

where

$$\begin{aligned} \Upsilon_1 = & (1 + \lambda_e^2 k^2) \frac{\omega^2}{V_A^2 k^2} - \frac{k_z^2}{k^2}, \\ \Upsilon_2 = & (1 + \lambda_e^2 k^2)^2 \frac{\omega^2}{V_A^2 k^2} - \frac{k_z^2}{k^2} + \frac{V_A^2 k_z^2}{\omega^2} - \lambda_i^2 k_z^2, \end{aligned}$$

The number density and the parallel magnetic field are related by

$$\frac{\delta n}{n_0} = - \frac{1}{\beta} \frac{k^2}{k_\perp^2} \frac{1 + \lambda_e^2 k^2 - \Upsilon_2}{1 + \lambda_e^2 k^2 - V_A^2 k_z^2 / \omega^2} \frac{\delta B_z}{B_0}. \quad (11)$$

These relations (7)–(11) can be used in the diagnostics of experimentally observed wave phenomena.

3. KAW PROPERTIES

KAWs behave differently in different β regimes, namely, the inertial regime $\beta < m_e/m_i$, the kinetic regime $m_e/m_i < \beta < 1$, and the high- β regime $\beta \gtrsim 1$. Thus, we will investigate the KAW properties for the representative values $\beta = 10^{-4}$, typical in the Earth's ionosphere and the solar flare loops, $\beta = 10^{-2}$, typical in the Earth's magnetosphere and the solar corona, and $\beta = 1$, typical in the solar wind at ~ 1 AU.

From Figure 2 one can see that the KAW frequency is larger than the ion-cyclotron frequency, $\omega \gtrsim \omega_{ci}$, when $k_\perp \rho = 1$ and $\theta = 87^\circ$ or 89° , but $\omega/\omega_{ci} < 1$ for extremely oblique propagation, $\theta = 89^\circ.99$. This is consistent with the result in Sahraoui et al. (2012) that $\omega/\omega_{ci} < 1$ at all scales as the propagating angle $\theta > \theta_{\text{crit}} = \cos^{-1}(Q) \simeq 89^\circ.97$.

Figure 3 presents the electric polarization of KAWs. The waves are polarized elliptically (almost linearly in low- β plasmas), $P_{\delta E, \mathbf{B}_0} = \delta E_y / (i \delta E_x) < 1$. At relatively small ρk_\perp , the polarization parameter is positive,

$P_{\delta E, \mathbf{B}_0} > 0$, in the kinetic and high- β regimes, which corresponds to the right-hand polarization, as was first shown by (Gary 1986; Hollweg 1999). However, at larger $\rho k_\perp > 1$ there are several transition points where δE_x passes through zero and $\delta E_y / i \delta E_x$ and $\delta E_z / \delta E_x$ change their signs. These polarization reversals are discussed in more detail below.

Figures 4 and 5 show the magnetic polarization and the magnetic helicity σ of KAWs. At the ion scale $\rho k_\perp \sim 1$ we observe quite small $i \delta B_x / \delta B_y \sim 0.01$, but the values of $i \delta B_z / \delta B_y$ are larger. For $\rho k_\perp \lesssim 1$ the KAW helicity is right-hand ($\sigma < 0$) in the inertial regime but becomes left-hand at larger β (it also becomes left-hand in the inertial range at larger ρk_\perp).

Figure 6 presents the plasma-magnetic pressure correlation $C_{PBn} = \frac{\gamma(T_i + T_e) \delta n}{\delta B_z B_0 / \mu_0}$ and compressibility $C_{Bn} = \frac{\delta n^2 / n_0^2}{\delta B^2 / B_0^2}$ of KAWs. It is interesting to observe the pressure balance $C_{PBn} \simeq -1$ in the extremely oblique KAWs ($\theta = 89^\circ.99$) at arbitrary β . $C_{PBn} \simeq -1$ also holds for the arbitrary propagation angle in the high- β plasmas. Note several transition points in the inertial regime where C_{Bn} changes its sign, which occur when $k_z^2 / k_\perp^2 - (1 + \lambda_e^2 k_\perp^2) \beta = 0$. C_{Bn} nearly follows the approximate expression $C_{Bn} \simeq \rho^2 k_\perp^2 (1 + \lambda_e^2 k_\perp^2 + \lambda_i^2 k_z^2) / \beta (1 + \rho^2 k_\perp^2)$ that is valid for the low β .

Figure 7 presents the ion Alfvén ratio R_{Ai} and the ion cross helicity σ_{Ci} of KAWs. R_{Ai} and σ_{Ci} can be rewritten as $R_{Ai} = \delta v_i^2 / \delta v_B^2$ and $\sigma_{Ci} = 2(\delta \mathbf{v}_i \cdot \delta \mathbf{v}_B^*) / (\delta v_i^2 + \delta v_B^2)$, where δv_B is the magnetic perturbation in the units of Alfvén speed. The ion cross-helicity becomes nearly zero, $\sigma_{Ci} \sim 0$, as the strong velocity mismatch appears, $\delta v_i \gg \delta v_B$ (for the kinetic scale $\lambda_e k_\perp > 1$ waves with $\rho k_\perp > 10^{-2}$ in the inertial regime) or $\delta v_B \gg \delta v_i$ (for KAWs with $\rho k_\perp > 1$ in the high- β plasmas).

In the following sub-sections we consider the electric field polarization and its reversal in more detail.

3.1. Electric Polarization and Its Reversal

In the limit $k_\perp \gg k_z$, from the expression (8) we get the polarization ratio

$$\frac{\delta E_y}{\delta E_x} = i \frac{\omega}{\omega_{ci}} \frac{1}{\lambda_i^2 k_\perp^2} \frac{(1 + \lambda_e^2 k_\perp^2) \frac{\omega^2}{V_A^2 k_z^2} - 1}{\tilde{T}_i (1 + \lambda_e^2 k_\perp^2) \frac{\omega^2}{V_A^2 k_z^2} + \tilde{T}_e \left(1 - \frac{\omega^2}{\omega_{ci}^2} \right)}. \quad (12)$$

The sense of the wave polarization can change when the numerator or denominator of this expression passes through zero, which correspond to $\delta E_y = 0$ or $\delta E_x = 0$, respectively. The $\delta E_x = 0$ transition occurs at

$$\left(\frac{\omega^2}{\omega_{ci}^2} - 1 \right) = \frac{\tilde{T}_i}{\tilde{T}_e} (1 + \lambda_e^2 k_\perp^2) \frac{\omega^2}{V_A^2 k_z^2} > 0, \quad (13)$$

which implies high-frequency $\omega > \omega_{ci}$ waves at the transition point. For the low-frequency waves ($\omega \ll \omega_{ci}$), there are no such transition points. In low- β limit this transition can occur as

$$\lambda_i^2 k_z^2 = \frac{(1 + \lambda_e^2 k_\perp^2) \left(1 + (1 + \rho^2 k_\perp^2) \frac{\tilde{T}_i}{\tilde{T}_e} \right)}{\rho^2 k_\perp^2}. \quad (14)$$

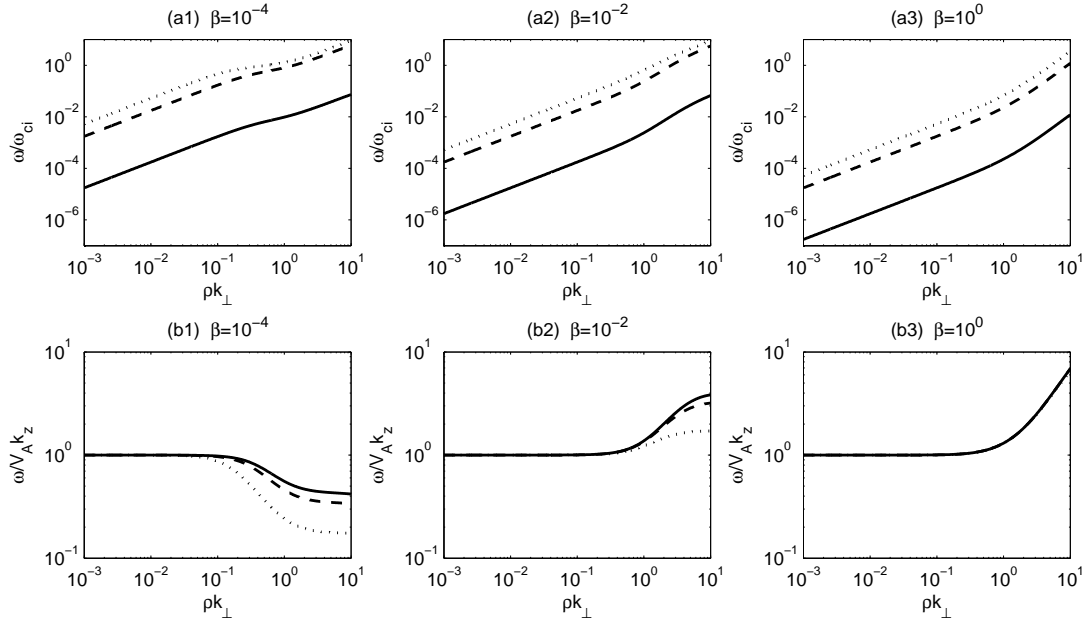


FIG. 2.— Wave frequency of KAWs in three different β regimes: inertial regime $\beta = 10^{-4}$, kinetic regime $\beta = 10^{-2}$, and high- β regime $\beta = 1$. The dotted, dashed, and solid lines represent the propagating angle $\theta = 87^\circ$, 89° , and $89^\circ.99$, respectively. (a) ω is normalized by ω_{ci} ; (b) ω normalized by $V_A k_z$. The equal electron and ion temperatures, $T_e = T_i$, is used here and following figures.

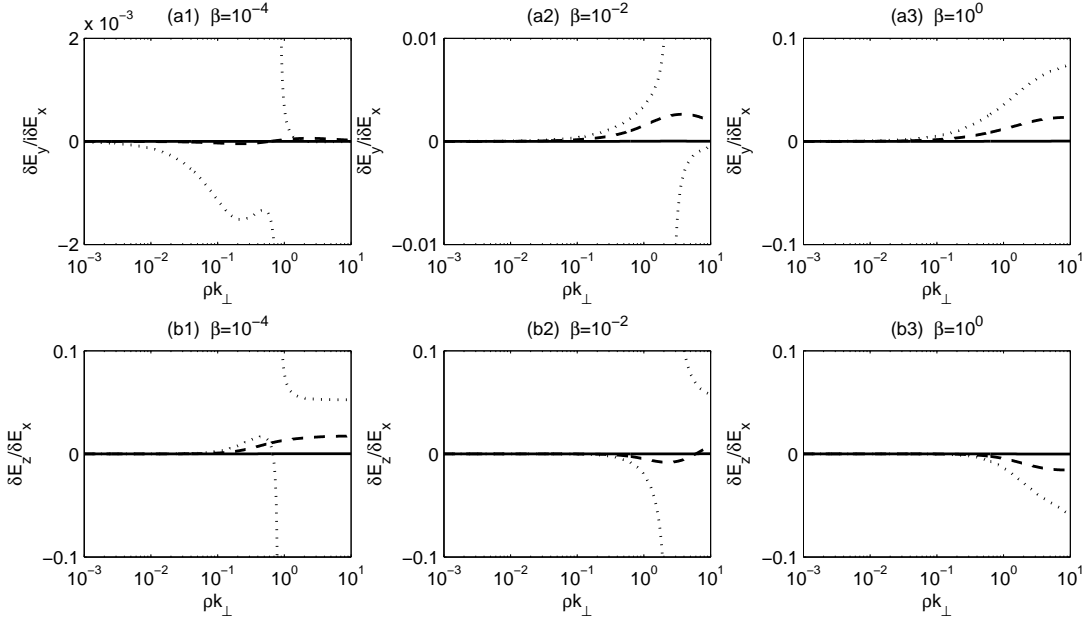


FIG. 3.— Electric polarization ratios $\delta E_y/(i\delta E_x)$ and $\delta E_z/\delta E_x$ for KAWs. The dotted, dashed, and solid lines represent the propagating angles $\theta = 87^\circ$, 89° , and $89^\circ.99$, respectively.

The $\delta E_y = 0$ transition occurs at

$$\frac{\omega^2}{V_A^2 k_z^2} = \frac{1}{1 + \lambda_e^2 k_\perp^2} < 1. \quad (15)$$

This transition implies sub-Alfvénic phase velocities of KAWs and is possible only due to finite $\lambda_e^2 k_\perp^2$. In low- β limit (15) gives the transition wavenumber

$$\rho^2 k_{\perp \text{tr}}^2 = \frac{m_i}{m_e} \left(\frac{1}{\tan^2 \theta} - \beta \right). \quad (16)$$

With growing $\rho^2 k_\perp^2$, the transition occurs from the left-

to right-hand polarization. For this transition to occur, the wave propagation angle should be less than certain value,

$$\theta < \theta_{\text{cr}} = \arctan \frac{1}{\sqrt{\beta}}. \quad (17)$$

Otherwise, the wave is always right-hand polarization. Only in this last case the conclusion by (Gary 1986; Hollweg 1999) holds that KAWs are right-hand polarized.

The above analysis indicates that KAWs can be both left- and right-hand polarized.

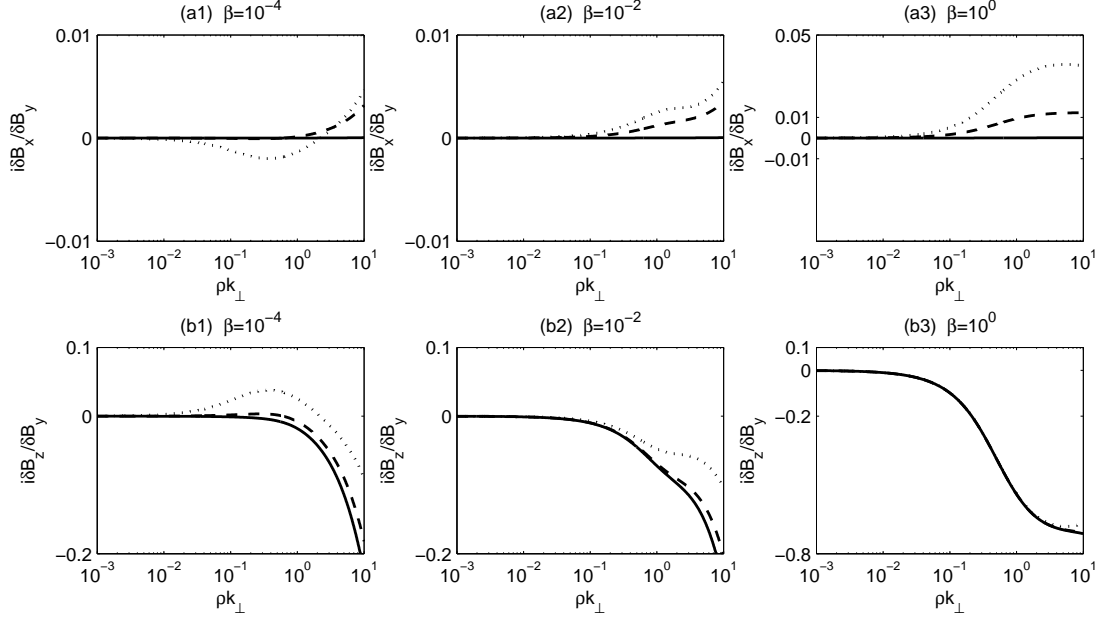


FIG. 4.— Magnetic polarization ratios $i\delta B_x/\delta B_y$ and $i\delta B_z/\delta B_y$ for KAWs. The dotted, dashed, and solid lines represent the wave propagation angles $\theta = 87^\circ$, 89° , and $89^\circ.99$, respectively.

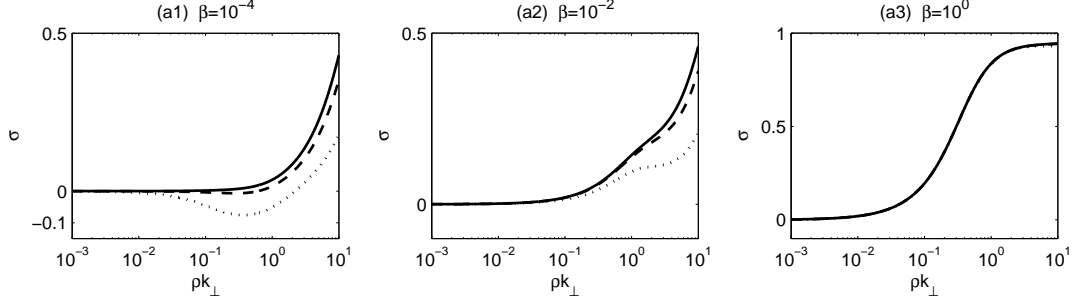


FIG. 5.— Magnetic helicity σ of KAWs. The dotted, dashed, and solid lines represent the propagation angles $\theta = 87^\circ$, 89° , and $89^\circ.99$, respectively.

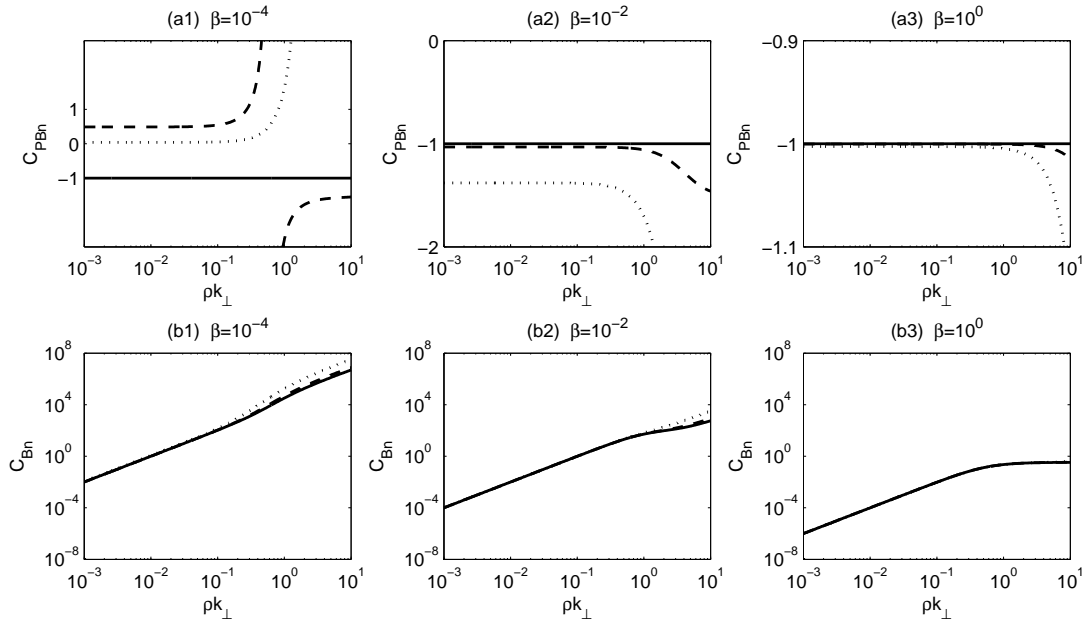


FIG. 6.— Pressure correlation C_{PBn} and compressibility C_{Bn} of KAWs. The dotted, dashed, and solid lines represent the propagation angles $\theta = 87^\circ$, 89° , and $89^\circ.99$, respectively.

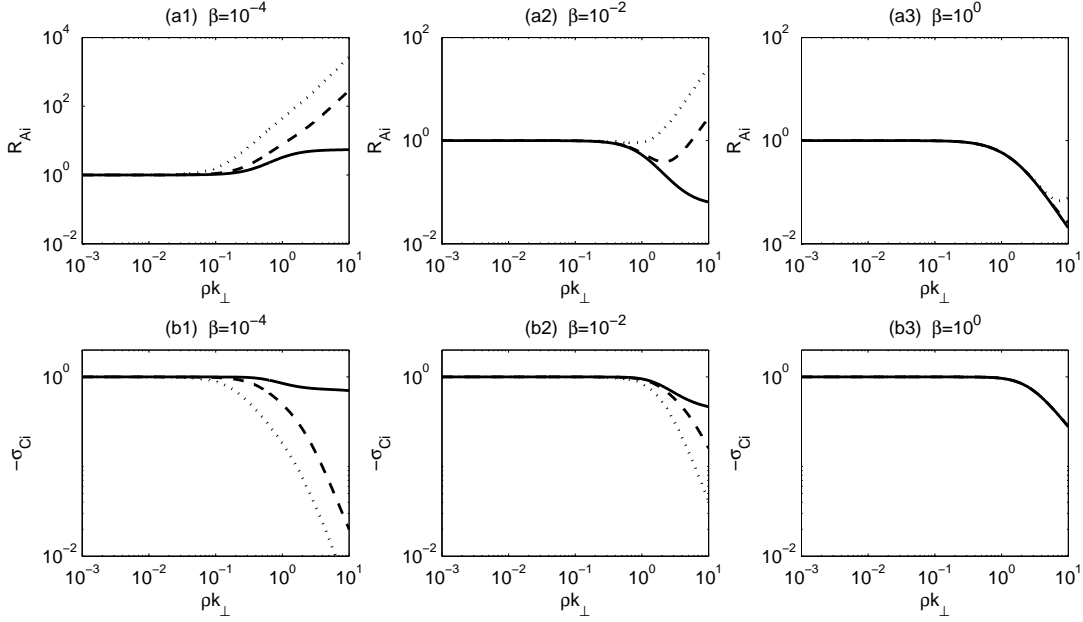


FIG. 7.— Ion Alfvén ratio R_{Ai} and cross helicity σ_{Ci} of KAWs. The dotted, dashed, and solid lines represent the propagation angles $\theta = 87^\circ, 89^\circ, 89^\circ.99$, respectively.

3.2. The Low- β Low-frequency Limit

For KAWs in low- β plasmas, $\beta \ll 1$, we get

$$\frac{\delta E_y}{\delta E_x} = i\beta \frac{\omega}{\omega_{ci}} \frac{1}{1 + \rho_i^2 k_\perp^2} \frac{(1 + \lambda_e^2 k_\perp^2) - \lambda_i^2 k_z^2 / \rho^2 k_\perp^2}{(1 + \lambda_e^2 k_\perp^2) - \lambda_i^2 k_z^2 \rho_s^2 k_\perp^2 / (1 + \rho_i^2 k_\perp^2)}. \quad (18)$$

At small $\lambda_i^2 k_z^2 \ll 1$ (i.e. in the low-frequency range) the denominator of the above expression is dominated by the term $(1 + \lambda_e^2 k_\perp^2)$, and we arrive to

$$\frac{\delta E_y}{\delta E_x} = i\beta \frac{\omega}{\omega_{ci}} \frac{1}{1 + \rho_i^2 k_\perp^2} \left(1 - \frac{1}{\left(\beta + \frac{m_e}{m_i} \rho^2 k_\perp^2 \right) \tan^2 \theta} \right), \quad (19)$$

which indicates that the electric polarization depends on the magnitude of k_\perp compared to the ion kinetic scales. In the limit $\beta \tan^2 \theta \gg 1$, our expression (19) simplifies to

$$\frac{\delta E_y}{\delta E_x} = i\beta \frac{\omega}{\omega_{ci}} \frac{1}{1 + \rho_i^2 k_\perp^2}. \quad (20)$$

In this limit the waves are always right-hand polarized. In principle, this conclusion agrees with previous results (Gary 1986; Hollweg 1999). In the long-wavelength limit $\rho_i^2 k_\perp^2 \ll 1$, Equation (19) reduces to the approximate analytical formula Equation (46) by (Hollweg 1999),

$$\frac{\delta E_x}{\delta E_y} = i\beta \frac{\omega}{\omega_{ci}}. \quad (21)$$

4. KSW PROPERTIES

Before discussing properties of the oblique slow waves in the two-fluid MHD, it is instructive to mention some their known properties in the kinetic theory. At general oblique propagation, the slow/sound wave extends to the frequency larger than the ion cyclotron frequency as showed in Figure 1 by Krauss-Varban et al. (1994) for the propagation angle $\theta = 30^\circ$. At larger propagation angles,

large wavenumbers are required for the waves to reach the ion-cyclotron frequency, and for quasi-perpendicular propagation slow waves remain sub-cyclotron in the wide range of perpendicular wavenumber, up to large values of $\rho^2 k_\perp^2$. In the two-fluid MHD, the frequency of quasi-perpendicular KSWs always remains sub-cyclotron:

$$\frac{\omega}{\omega_{ci}} = \frac{k_z}{k_\perp} \sqrt{\frac{\rho^2 k_\perp^2}{1 + \rho^2 k_\perp^2}} < 1 \quad \text{for} \quad \frac{k_z}{k_\perp} \leq 1.$$

The KSW dispersion is showed in Figure 8 in terms of the phase velocity $\omega/(V_T k_z)$, which exhibits also a depression at high β in the long-wavelength limit.

Figure 9 presents the electric polarization of KSWs. The polarization parameter $P_{E,B_0} = E_y/(i\delta E_x) < 0$ means the left-hand KSW polarization. δE_x becomes the dominant component for the waves at the ion gyroradius scale ($\rho k_\perp \sim 1$). The KSW electric field polarization ratios can be approximated as $i\delta E_y/\delta E_x \simeq \beta k_z / (\rho k_\perp^2 \sqrt{1 + \rho^2 k_\perp^2})$, and $\delta E_z/\delta E_x = k_z/k_\perp$.

Figure 10 presents the magnetic polarization of KSWs. For the long wavelength waves ($\rho k_\perp \ll 1$), the compressible magnetic field perturbation δB_z is the dominant component, $|\delta B_z/\delta B_{x,y}| \gg 1$. However, δB_y becomes as important as δB_z when the wavelength approaches the ion gyroradius scale, where $\delta B_y \simeq \delta B_z \gg \delta B_x$. The magnetic field polarization ratios nearly follow the approximate relations $i\delta B_x/\delta B_y = -(k_z/k_\perp) \sqrt{1 + 1/\rho^2 k_\perp^2}$ and $i\delta B_z/\delta B_y = \sqrt{1 + 1/\rho^2 k_\perp^2}$.

The helicity σ in the low- β plasmas can be written as $\sigma = -2\rho k_\perp (1 + \rho^2 k_\perp^2)^{1/2} / (1 + 2\rho^2 k_\perp^2)$, which indicates that σ decreases from 0 to -1 as ρk_\perp increases from 10^{-3} to 10. This behavior is seen from Figure 11.

Figure 12 presents the plasma/magnetic pressure correlation C_{PBn} and the compressibility C_{Bn} of KSWs. The behavior of these functions is in accordance with the theoretic predictions that $C_{PBn} \simeq -1$ and $C_{Bn} \simeq$

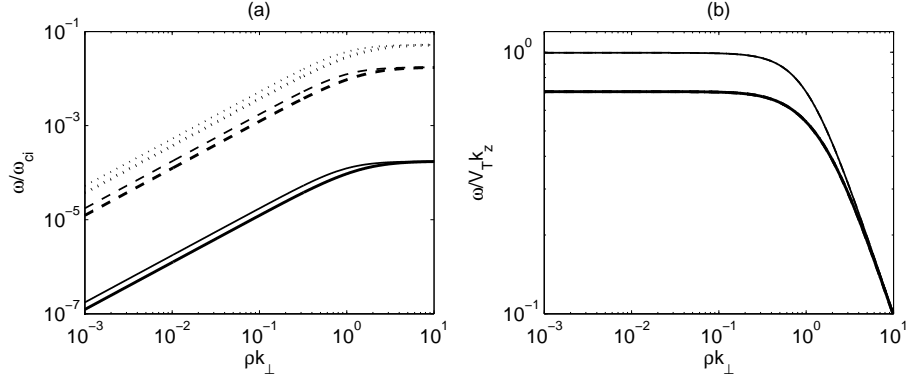


FIG. 8.— Wave frequency of KSWs in three different β regimes, the inertial regime ($\beta = 10^{-4}$, the thin lines), the kinetic regime ($\beta = 10^{-2}$, the middle lines), and the high- β regime ($\beta = 1$, the thick lines), where the dotted, dashed, and solid lines represent the propagating angles $\theta = 87^\circ$, 89° , and $89^\circ.99$, respectively. The lines in the inertial regime are the same as in the kinetic regime. (a) ω is normalized by ω_{ci} ; (b) ω normalized by $V_T k_z$.

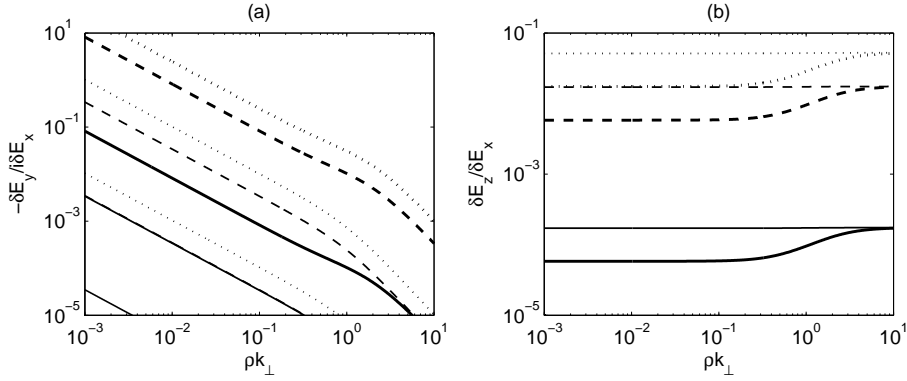


FIG. 9.— Electric-field polarization $\delta E_y / (i \delta E_x)$ and $\delta E_z / \delta E_x$ of KSWs, where the lines have the same meaning as in Figure 8.

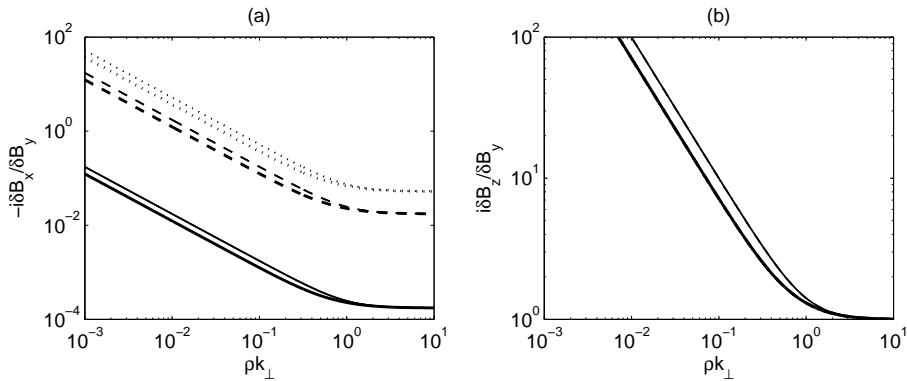


FIG. 10.— Magnetic-field polarization $i \delta B_x / \delta B_y$ and $\delta B_z / \delta B_y$ of KSWs, where the lines have the same meaning as in Figure 8.

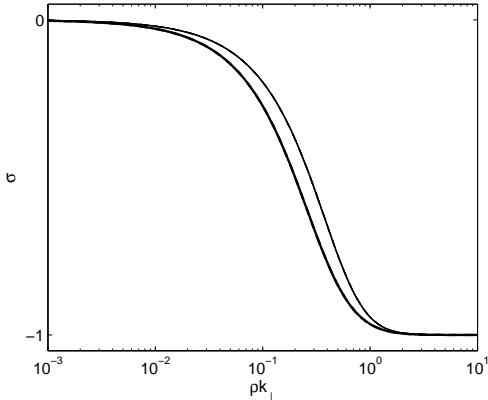


FIG. 11.— Magnetic helicity of KSWs. The lines have the same meaning as in Figure 8.

$(1 + \rho^2 k_{\perp}^2) / (1 + 2\rho^2 k_{\perp}^2) / \beta^2$ in the low- β plasma. Note that C_{PBn} and C_{Bn} in the high- β plasmas can be approximated by the same expressions.

Figure 13 presents the ion Alfvén ratio R_{Ai} and the cross-helicity σ_{Ci} of KSWs. δv_i is nearly equal δv_B in the long-wavelength waves ($\rho k_{\perp} \ll 1$) in high- β plasmas. In other cases δv_i dominates over δv_B , $\delta v_i > \delta v_B$. The corresponding expressions in the low- β plasmas are $R_{Ai} \simeq (1 + 2\rho^2 k_{\perp}^2) / \beta$ and $\sigma_{Ci} \simeq -2\sqrt{\beta} / (1 + \rho^2 k_{\perp}^2)$.

5. DISCUSSION AND CONCLUSION

Our study shows that the Alfvén wave frequency ω at the ion gyroscale $\rho k_{\perp} \sim 1$ is smaller than the ion-cyclotron frequency ω_{ci} for extremely oblique propagation, say for $\theta = 89^\circ.99$. In agreement with (Sahraoui et al. 2012), the KAW frequency can reach ω_{ci} for propagation angle $\theta \leq 89^\circ.97$. At $\rho k_{\perp} \sim 1$, ω can reach and exceed ω_{ci} for the propagation angles $\sim 87^\circ$ or less. At smaller propagating angles, the frequency $\omega \sim \omega_{ci}$ occurs at smaller wavenumbers. In the solar-terrestrial plasmas, the high-frequency KAWs may be generated through the Alfvénic turbulent cascade (Huang et al. 2012), excited kinetically by the field-aligned currents and ion beams (Voitenko & Goossens 2002; Voitenko & Goossens 2003), or by phase mixing combined with cyclotron sweep of Alfvén waves (Voitenko & Goossens 2006).

Our study investigated KAWs and KSWs in a wide range of β , covering a wide range of conditions in most solar-terrestrial plasmas. Several mode properties of KAWs are totally different in the limits $\beta < m_e/m_i$ (so-called inertial range) and $\beta > m_e/m_i$ (kinetic range). So, we confirmed that the KAW phase velocity ω/k_z in the inertial range decreases with increasing k_{\perp} , but increases in the kinetic and high- β ranges (Goertz & Boswell 1979; Lysak & Lotko 1996; Stasiewicz et al. 2000). The electric polarization ratios of KAWs are also obviously different in these two distinct β ranges. Namely, except for the case of extremely oblique waves, at smaller k_{\perp} KAWs are left-hand polarized in the inertial range and right-hand in the kinetic/high- β ranges. The magnetic helicity at these wavenumbers is right-hand for $\beta < m_e/m_i$ and left-hand for $\beta > m_e/m_i$. At higher k_{\perp} they undergo two polarization reversals defined by (13) and (15). These new polarization properties of KAWs, especially polarization reversals, are quite specific and can be used

as a critical test for the mode identification in the solar wind and terrestrial magnetosphere. In addition to the Landau dissipation caused by the parallel electric field fluctuations of KAWs, the perpendicular electric field can induce the occurrence of the cyclotron resonant damping as the frequency of KAWs reaches or exceeds the ion cyclotron frequency (Voitenko & Goossens 2002, 2003). The cyclotron-resonant damping (Kennel & Wong 1967; Marsch 2006) does not require purely left-hand or purely right-hand polarizations of Alfvén waves. When the resonant-cyclotron condition $\omega(k_z) - k_z v_z = n\omega_{ci}$ is satisfied for the oblique waves, there are two resonance cases depending on the interaction with E_x or E_y (Hollweg & Markovskii 2002), where v_z is the parallel velocity of particles. E_x can cause the cyclotron resonance if the particles stay in the phase with the waves, whereas the resonance relating to E_y strongly depends on the x-position of the particles (Hollweg & Markovskii 2002). Both Landau and cyclotron dampings are crucial when investigating the turbulence dissipation channels at kinetic scales. On the contrary, the KSWs properties are nearly the same in all β ranges and can be approximately described by the approximate expressions for the low- β plasmas given in Section 4.

Our study provided a clear evidence of anti-correlation between the plasma and magnetic pressures for both KAWs and KSWs in high- β plasmas. This makes the total pressure fluctuations almost zero, $\delta P_{tot} \simeq 0$, which resembles the main common property of the observed PBSs (Yao et al. 2011). Kellogg & Horbury (2005) and Yao et al. (2011) used the Cluster data, which have a high time resolution of 0.2 s for the plasma number density and magnetic field, and found that the scales of PBSs extend down to the ion scale. Kellogg & Horbury (2005) interpreted these kinetic-scale PBSs in terms of KSWs. However, KAWs may be an alternative explanation since they also drive anti-correlated number density and magnetic field fluctuations. Again, one needs more mode properties to discriminate which mode dominates in PBSs, KSW or KAW. Our results reveal three different properties that distinguish these modes at the ion gyroradius scale: (1) right-hand electric polarization for KAWs and left-hand for KSWs; (2) magnetic helicity $\sigma \sim 1$ for KAWs and $\sigma \sim -1$ for KSWs; (3) Alfvén ratio $R_{Ai} \ll 1$ for KAWs and $R_{Ai} \gg 1$ for KSWs. Besides, the large-scale Alfvén waves, permeating the solar wind, can nonlinearly excite simultaneous KSWs and KAWs (Zhao et al. 2014), which both can contribute to the observed PBSs. This implies that PBSs may be KSWs, or KAWs, or a mixture of KSWs and KAWs. A recent work (Hollweg et al. 2014) showed that the highly-oblique slow mode has the small variation of P_{tot} in the three-fluid plasmas consisting of fully-ionized hydrogen and a heavy ion drifting along the background magnetic field. Therefore, one needs addition tests for a more careful identification of the wave modes producing the observed kinetic-scale PBSs.

In summary, we revealed several new mode properties of KAWs and KSWs accounting for the kinetic effects of the ion and electron thermal pressure and inertia. For KAWs, their frequency can reach and exceed the ion cyclotron frequency at the ion kinetic scales, where both the thermal and the inertial ion effects are important. The polarization properties of KAWs are different in dif-

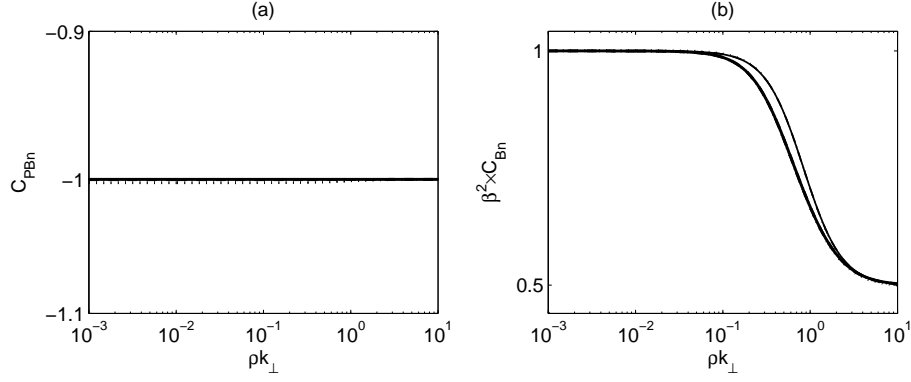


FIG. 12.— Plasma/magnetic pressure ratio C_{PBn} and compressibility C_{Bn} of KSWs. The lines have the same meaning as in Figure 8.

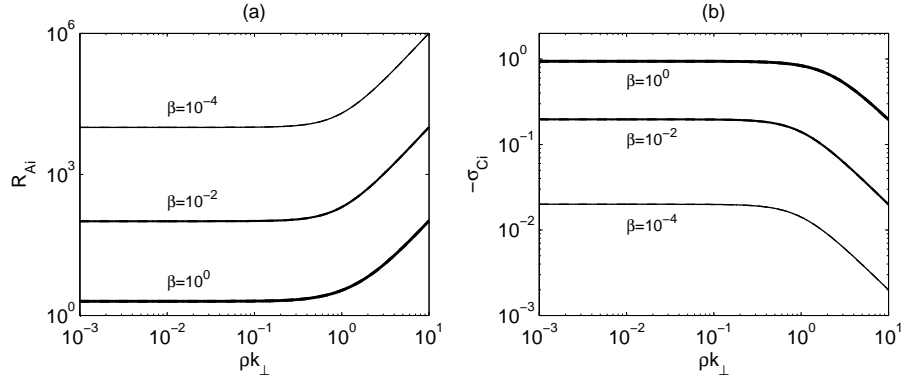


FIG. 13.— Ion Alfvén ratio R_{Ai} and cross-helicity σ_{Ci} of KSWs. The lines have the same meaning as in Figure 8.

ferent β ranges and depend on both the propagation angle θ and the normalized perpendicular wavenumber ρk_{\perp} . It appeared that KAWs undergo two reversals of electric polarization defined by the zeros of denominator (13) and the numerator (15) of (12). In particular, in low- β plasmas less oblique KAWs (17) are left-hand polarized at longer wavelengths and right-hand at shorter wavelengths. These properties are important for the turbulence cascade transition across the ion-cyclotron frequency, where it can be partially dissipated by the ion-cyclotron resonance, in such a way that the left-hand KAWs possess stronger dissipation as compared to the

right-hand ones.

For KSWs, its frequency is always smaller than ion cyclotron frequency and the mode is left-hand polarized. At the ion kinetic scales, $\rho k_{\perp} \sim 1$, the electric and magnetic KSW components obey $|\delta E_y| \ll |\delta E_x|$, $|\delta B_x| \ll |\delta B_y|$, and $|\delta B_z| \simeq |\delta B_y|$. All these properties of KSWs can be described approximately by the reduced expression obtained in the low- β limit.

These new properties are important for understanding short-wavelength Alfvén and slow modes and can be used in interpreting waves and turbulence at kinetic scales.

APPENDIX

A. THE GENERAL DISPERSION EQUATION

From the momentum Equation (1), the ion and electron velocities are found as

$$\Lambda_i \delta v_{ix} = -i \frac{\omega}{B_0 \omega_{ci}} \delta E_x + \frac{1}{B_0} \delta E_y - \frac{\gamma T_i \omega k_{\perp}}{m_i \omega_{ci}^2} \frac{\delta n}{n_0}, \quad (\text{A1})$$

$$\Lambda_i \delta v_{iy} = -\frac{1}{B_0} \delta E_x - i \frac{\omega}{B_0 \omega_{ci}} \delta E_y + i \frac{\gamma T_i k_{\perp}}{m_i \omega_{ci}} \frac{\delta n}{n_0}, \quad (\text{A2})$$

$$\delta v_{iz} = i \frac{e}{m_i \omega} \delta E_z + \frac{\gamma T_i k_z}{m_i \omega} \frac{\delta n}{n_0}, \quad (\text{A3})$$

$$\Lambda_e \delta v_{ex} = i \frac{Q\omega}{B_0 \omega_{ce}} \delta E_x + \frac{1}{B_0} \delta E_y - \frac{Q\gamma T_e \omega k_{\perp}}{m_e \omega_{ce}^2} \frac{\delta n}{n_0}, \quad (\text{A4})$$

$$\Lambda_e \delta v_{ey} = -\frac{1}{B_0} \delta E_x + i \frac{Q\omega}{B_0 \omega_{ce}} \delta E_y - i \frac{\gamma T_e k_{\perp}}{m_e \omega_{ce}} \frac{\delta n}{n_0}, \quad (\text{A5})$$

$$\delta v_{ez} = -i \frac{e}{m_e \omega} \delta E_z + \frac{\gamma T_e k_z}{m_e \omega} \frac{\delta n}{n_0}, \quad (\text{A6})$$

where $Q \equiv m_e/m_i$, $\Lambda_i \equiv 1 - \omega^2/\omega_{ci}^2$, and $\Lambda_e \equiv 1 - Q^2\omega^2/\omega_{ci}^2$. Note that the quasi-neutrality condition, $\delta n_i = \delta n_e \equiv \delta n$, has been used in last derivation. By the use of expressions (A1)–(A6), the current density $\delta \mathbf{J} = n_0 e (\delta \mathbf{v}_i - \delta \mathbf{v}_e)$ can be presented in the following form:

$$\Lambda_i \Lambda_e \delta J_x = -i \frac{n_0 e \omega}{B_0 \omega_{ci}} (\Lambda_e + Q \Lambda_i) \delta E_x + \frac{n_0 e}{B_0} (\Lambda_e - \Lambda_i) \delta E_y - \frac{\gamma T \omega k_\perp}{B_0 \omega_{ci}} (\Lambda_e \tilde{T}_i - Q \Lambda_i \tilde{T}_e) \delta n, \quad (\text{A7})$$

$$\Lambda_i \Lambda_e \delta J_y = -\frac{n_0 e}{B_0} (\Lambda_e - \Lambda_i) \delta E_x - i \frac{n_0 e \omega}{B_0 \omega_{ci}} (\Lambda_e + Q \Lambda_i) \delta E_y + i \frac{\gamma T k_\perp}{B_0} (\Lambda_e \tilde{T}_i + \Lambda_i \tilde{T}_e) \delta n, \quad (\text{A8})$$

$$\delta J_z = i (1 + Q) \frac{n_0 e^2}{m_e \omega} \delta E_z - \frac{e \gamma T k_z}{m_e \omega} (\tilde{T}_e - Q \tilde{T}_i) \delta n, \quad (\text{A9})$$

where $T = T_i + T_e$ and $\tilde{T}_{i,e} \equiv T_{i,e}/T$.

On the other hand, the current density can be expressed in terms of the perturbed electric field only,

$$\delta J_x = -i \frac{k_z^2}{\mu_0 \omega} \delta E_x + i \frac{k_\perp k_z}{\mu_0 \omega} \delta E_z, \quad (\text{A10})$$

$$\delta J_y = -i \frac{k^2}{\mu_0 \omega} \delta E_y, \quad (\text{A11})$$

$$\delta J_z = i \frac{k_\perp k_z}{\mu_0 \omega} \delta E_x - i \frac{k_\perp^2}{\mu_0 \omega} \delta E_z. \quad (\text{A12})$$

From Equations (A7) – (A12), the electric field components can be expressed in terms of δn :

$$\Pi \delta E_x = i k_\perp \frac{\gamma T}{e} \Pi_x \frac{\delta n}{n_0}, \quad (\text{A13})$$

$$\Pi \delta E_y = k_\perp \frac{\gamma T}{e} \Pi_y \frac{\delta n}{n_0}, \quad (\text{A14})$$

$$\Pi \delta E_z = i k_z \frac{\gamma T}{e} \Pi_z \frac{\delta n}{n_0}, \quad (\text{A15})$$

where

$$\begin{aligned} \Pi &= (1 + Q)^2 (1 + Q + \lambda_e^2 k_\perp^2) \omega^4 \\ &\quad - (1 + Q) [1 + Q + \lambda_e^2 k_\perp^2 + (1 + Q) k_z^2/k^2] \Lambda_h V_A^2 k^2 \omega^2 \\ &\quad + (1 + Q) \Lambda_i \Lambda_e V_A^4 k^2 k_z^2, \\ \Pi_x &= (1 + Q) (1 + Q + \lambda_e^2 k_\perp^2) (Q \tilde{T}_i - \tilde{T}_e) \omega^4 \\ &\quad - \left[(1 + Q + \lambda_e^2 k_\perp^2) (\Lambda_e \tilde{T}_i - Q \Lambda_i \tilde{T}_e) + (1 + Q) \Lambda_h (Q \tilde{T}_i - \tilde{T}_e) k_z^2/k^2 \right] V_A^2 k^2 \omega^2 \\ &\quad + \Lambda_i \Lambda_e (Q \tilde{T}_i - \tilde{T}_e) V_A^4 k^2 k_z^2, \\ \Pi_y &= (1 + Q) [(1 + Q + \lambda_e^2 k_\perp^2) \omega^2 - \Lambda_h V_A^2 k_z^2] \omega \omega_{ci}, \\ \Pi_z &= \Pi_x + (1 - Q^2) V_A^2 k^2 \omega^2, \end{aligned}$$

and $\Lambda_h \equiv (1 - Q\omega^2/\omega_{ci}^2)$.

Now we can use expressions (A13)–(A15) to eliminate the electric field from the number density equation

$$\left[(\Lambda_i + \rho_i^2 k_\perp^2) \omega^2 - \Lambda_i V_{Ti}^2 k_z^2 \right] \frac{\delta n}{n_0} = -i \frac{\omega^2 k_\perp}{B_0 \omega_{ci}} \delta E_x + \frac{\omega k_\perp}{B_0} \delta E_y + i \frac{e}{m_i} k_z \Lambda_i \delta E_z, \quad (\text{A16})$$

which results in the general dispersion equation:

$$\begin{aligned} &\omega^6 (1 + Q) (1 + Q + \lambda_e^2 k^2)^2 \\ &\quad - \omega^4 \left[(1 + Q) (1 + Q + \lambda_e^2 k^2) + (1 + Q + \lambda_e^2 k^2)^2 V_T^2/V_A^2 + (1 + Q^3) \lambda_i^2 k_z^2 + (1 + Q)^2 k_z^2/k^2 \right] V_A^2 k^2 \\ &\quad + \omega^2 \left[(1 + Q) (1 + 2V_T^2/V_A^2) + (1 + Q^2) \rho^2 k^2 \right] V_A^4 k^2 k_z^2 \\ &\quad - \beta V_A^6 k^2 k_z^4 = 0, \end{aligned} \quad (\text{A17})$$

where $V_T = \sqrt{\gamma T/m_i}$, $\rho^2 = \rho_i^2 + \rho_s^2$, ρ_i is the ion gyroradius, ρ_s is the ion-acoustic gyroradius, and λ_i is the ion inertial length.

In deriving Equation (A17), we neglected the displacement current in the Ampere's law, but kept all other terms. Also, we treated the electrons and ions separately. This makes our derivation and results different from the derivations by Stringer (1963) and Bellan (2012). The above two authors used equations of the mass motion and the generalized Ohm's law (Equations (A1) and (A2) in Stringer (1963)) with one-fluid variables $\rho = \sum_{\alpha=i,e} m_\alpha n_\alpha$ and $v = \sum_{\alpha=i,e} m_\alpha n_\alpha v_\alpha / \sum_{\alpha=i,e} m_\alpha n_\alpha$ where some terms of order Q were discarded. The resulting general dispersion equation is (Stringer, 1963)

$$\begin{aligned} & \omega^6 (1 + \lambda_e^2 k^2)^2 \\ & - \omega^4 \left[(1 + \lambda_e^2 k^2) + (1 + \lambda_e^2 k^2)^2 V_T^2 / V_A^2 + (1 + Q) \lambda_i^2 k_z^2 + k_z^2 / k^2 \right] V_A^2 k^2 \\ & + \omega^2 \left[(1 + 2V_T^2 / V_A^2) + (1 + 2Q) \rho^2 k^2 \right] V_A^4 k^2 k_z^2 \\ & - \beta V_A^6 k^2 k_z^4 = 0. \end{aligned} \quad (\text{A18})$$

Some terms in our expression (A17) and in Stringer's expression (A18) are different. The differences come from the different treatment of some minor terms $\sim Q$: all small terms are kept in our derivation but an incomplete set of terms was used by Stringer (1963). Since the major terms in Equations (A17) and (A18) are the same, the resulting dispersion relations for the fast, Alfvén and slow modes are also nearly the same. However, behavior of some polarization ratios differ significantly.

B. POLARIZATION AND CORRELATION

The wave properties involving wave polarization and correlation are summarized in (Krauss-Varban et al. 1994), here we repeat these definitions for convenient discussion. The electric field polarization with respect to the ambient magnetic-field is defined as

$$P_{E,\mathbf{B}_0} = \frac{\delta E_y}{i\delta E_x}. \quad (\text{B1})$$

The right-hand polarized mode corresponds to $\text{Re}(P_{E,\mathbf{B}_0}) > 0$, and left-hand polarized mode corresponds to $\text{Re}(P_{E,\mathbf{B}_0}) < 0$. $\text{Rm}(P_{E,\mathbf{B}_0}) = \pm 1$ correspond to the right- or left-hand circularly polarized mode. Note that the definition $P_{E,\mathbf{B}_0} = i\delta E_x / \delta E_y$ is used in (Krauss-Varban et al. 1994).

The magnetic field polarization with respect to the ambient magnetic-field is defined as

$$P_{B,\mathbf{B}_0} = \frac{\delta B_y}{i\delta B_x}, \quad (\text{B2})$$

and the magnetic field polarization with respect to wave vector is

$$P_{B,\mathbf{k}} = \frac{i\delta\mathbf{B} \cdot (\hat{\mathbf{z}} \times \hat{\mathbf{e}}_y)}{\delta B_y} = \frac{1}{P_{\delta B,\mathbf{B}_0} \cos\theta}. \quad (\text{B3a})$$

The magnetic helicity is expressed as

$$\sigma = \frac{k(\mathbf{A} \cdot \delta\mathbf{B}^*)}{\delta B^2} = \frac{2\text{Re}(P_{B,\mathbf{k}})}{1 + |P_{B,\mathbf{k}}|^2}, \quad (\text{B4})$$

where positive or negative helicity corresponds to a left- or right-hand sense of rotation with respect to \mathbf{k} (Gary 1986), respectively.

The magnetic field – density correlation corresponds to

$$C_{\parallel} = \frac{\delta n / n_0}{\delta B_z / B_0}, \quad (\text{B5})$$

Correspondingly, the thermal pressure – magnetic pressure correlation is defined as

$$C_{PBn} = \frac{\gamma(T_i + T_e) \delta n}{\delta B_z B_0 / \mu_0} = \beta C_{\parallel}, \quad (\text{B6})$$

hence, the total pressure perturbation is written as $\delta P_{tot} = (1 + \beta C_{\parallel}) \delta B_z B_0 / \mu_0$.

Compressibility

$$C_{Bn} = \frac{\delta n^2 / n_0^2}{\delta B^2 / B_0^2} = \sin^2\theta |C_{\parallel}|^2 \frac{|P_{\delta B,\mathbf{k}}|^2}{1 + |P_{\delta B,\mathbf{k}}|^2}, \quad (\text{B7})$$

describes the relation between the total magnetic field perturbation and the number density.

The Alfvén ratio and cross helicity for j species are defined as

$$R_A^j = \mu_0 n_0 m_i \frac{|\delta \mathbf{v}_j|^2}{|\delta \mathbf{B}|^2}, \quad (\text{B8})$$

$$\sigma_C^j = 2 \frac{(\mu_0 n_0 m_i)^{1/2} \text{Re}(\delta \mathbf{v}_j \cdot \delta \mathbf{B}^*)}{\mu_0 n_0 m_i |\delta \mathbf{v}_j|^2 + |\delta \mathbf{B}|^2}, \quad (\text{B9})$$

which gives the correlation between the perturbed velocity and magnetic field.

C. LINEAR DISPERSION AND WAVE PARAMETERS IN THE LOW- β PLASMA

In the low-beta plasma, $\beta \ll 1$, the linear dispersion and relations among field and plasma quantities are simpler than (6)–(7). For KAWs, the dispersion relation

$$\omega^2 = V_A^2 k_z^2 \mathcal{R} / \mathcal{L}', \quad (\text{C1})$$

and

$$\begin{aligned} \frac{\delta \mathbf{E}}{V_A} &= \frac{\mathcal{R}_i \mathcal{L} - \rho_s^2 k_\perp^2 \lambda_i^2 k_z^2}{\mathcal{R}^{1/2} \mathcal{L}'^{1/2}} \delta B_y \hat{\mathbf{e}}_x + i \frac{k_z}{k_\perp} \frac{(\mathcal{L} \rho^2 k_\perp^2 - \lambda_i^2 k_z^2)}{\lambda_i k_\perp \mathcal{L}'} \delta B_y \hat{\mathbf{e}}_y - \frac{k_z}{k_\perp} \frac{(1 + \lambda_i^2 k_z^2) \rho_s^2 k_\perp^2 - \mathcal{R}_i \lambda_e^2 k_\perp^2}{\mathcal{R}^{1/2} \mathcal{L}'^{1/2}} \delta B_y \hat{\mathbf{e}}_z, \\ \delta \mathbf{B} &= -i \frac{k_z}{k_\perp} \frac{(\mathcal{L} \rho^2 k_\perp^2 - \lambda_i^2 k_z^2)}{\lambda_i k_\perp \mathcal{R}^{1/2} \mathcal{L}'^{1/2}} \delta B_y \hat{\mathbf{e}}_x + \delta B_y \hat{\mathbf{e}}_y + i \frac{\mathcal{L} \rho^2 k_\perp^2 - \lambda_i^2 k_z^2}{\lambda_i k_\perp \mathcal{R}^{1/2} \mathcal{L}'^{1/2}} \delta B_y \hat{\mathbf{e}}_z, \\ \frac{\delta \mathbf{v}_i}{V_A} &= -i \lambda_i k_z \frac{\delta B_y}{B_0} \hat{\mathbf{e}}_x - \frac{\mathcal{L}'^{1/2}}{\mathcal{R}^{1/2}} \frac{\delta B_y}{B_0} \hat{\mathbf{e}}_y - i \frac{(\mathcal{R} - \mathcal{L} + \rho^2 k_\perp^2 \lambda_i^2 k_z^2)}{\lambda_i k_\perp \mathcal{R}} \frac{\delta B_y}{B_0} \hat{\mathbf{e}}_z, \\ \frac{\delta \mathbf{v}_e}{V_A} &= i \frac{k_z}{k_\perp} \frac{(\mathcal{L} \rho^2 k_\perp^2 - \lambda_i^2 k_z^2) \mathcal{R}}{\lambda_i k_\perp \mathcal{L}'} \frac{\delta B_y}{B_0} \hat{\mathbf{e}}_x - \frac{\mathcal{L} \mathcal{R}^{1/2}}{\mathcal{L}'^{1/2}} \frac{\delta B_y}{B_0} \hat{\mathbf{e}}_y - i \lambda_i k_\perp \frac{\delta B_y}{B_0} \hat{\mathbf{e}}_z, \end{aligned} \quad (\text{C2})$$

where

$$\mathcal{R} = 1 + \rho^2 k_\perp^2, \quad \mathcal{R}_i = 1 + \rho_i^2 k_\perp^2, \quad \mathcal{L} = 1 + \lambda_e^2 k_\perp^2, \quad \mathcal{L}' = 1 + \lambda_e^2 k_\perp^2 + \lambda_i^2 k_z^2.$$

For KSWs, the dispersion relation

$$\omega^2 = V_T^2 k_z^2 / \mathcal{R}, \quad (\text{C3})$$

and

$$\begin{aligned} \frac{\delta \mathbf{E}}{V_T} &= \frac{\mathcal{L} \tilde{T}_i + \mathcal{R} \tilde{T}_e / \beta}{\mathcal{R}^{1/2}} \delta B_y \hat{\mathbf{e}}_x - i \frac{k_z}{\rho k_\perp^2} \delta B_y \hat{\mathbf{e}}_y + \frac{k_z}{k_\perp} \frac{\mathcal{L} \tilde{T}_i + \mathcal{R} \tilde{T}_e / \beta - 1}{\mathcal{R}^{1/2}} \delta B_y \hat{\mathbf{e}}_z, \\ \delta \mathbf{B} &= i \frac{k_z}{\rho k_\perp^2} \mathcal{R}^{1/2} \delta B_y \hat{\mathbf{e}}_x + \delta B_y \hat{\mathbf{e}}_y - i \frac{\mathcal{R}^{1/2}}{\rho k_\perp} \delta B_y \hat{\mathbf{e}}_z, \\ \frac{\delta \mathbf{v}_i}{V_T} &= -i \frac{k_z (1 + \lambda_i^2 k_\perp^2)}{\rho k_\perp^2} \frac{\delta B_y}{B_0} \hat{\mathbf{e}}_x - \frac{\mathcal{R}^{1/2}}{\beta} \frac{\delta B_y}{B_0} \hat{\mathbf{e}}_y + i \frac{\mathcal{R}}{\beta \rho k_\perp} \frac{\delta B_y}{B_0} \hat{\mathbf{e}}_z, \\ \frac{\delta \mathbf{v}_e}{V_T} &= -i \frac{k_z}{\rho k_\perp^2} \frac{\delta B_y}{B_0} \hat{\mathbf{e}}_x - \frac{\mathcal{L}}{\mathcal{R}^{1/2}} \frac{\delta B_y}{B_0} \hat{\mathbf{e}}_y + i \frac{1}{\beta \rho k_\perp} \frac{\delta B_y}{B_0} \hat{\mathbf{e}}_z \end{aligned} \quad (\text{C4})$$

This research was supported by the Belgian Federal Science Policy Office via IAP Programme (project P7/08 CHARM), by the European Commission via FP7 Program (project 313038 STORM), by NSFC under grant No. 11303099, No.11373070, and No. 41074107, by MSTC under grant No. 2011CB811402, by NSF of Jiangsu Province under grant No. BK2012495, and by Key Laboratory of Solar Activity at NAO, CAS, under grant No. KLSA201304.

REFERENCES

- Bellan, P. M. 2012, JGR, 117, A12219
 Bellan, P. M. 2013, JGR, 118, 4435
 Bian, N. H., Kontar, E. P., & Brown, J. C. 2010, A&A, 519, 114
 Chaston, C. C., Salem, C., Bonnell, J. W., et al. 2008, PhRvL, 100, 175003
 Chaston, C. C., Johnson, J. R., Wilber, M., et al. 2009, PhRvL, 102, 015001
 Chen, L., & Wu, D. J. 2011, PhPl, 18, 072110
 Gary, S. P., 1986, JPIPh, 35, 431
 Goertz, C. K., & Boswell, R. W. 1979, JGR, 84, 7239
 He, J., Tu, C., Marsch, E., & Yao, S. 2012, ApJ, 749, 86
 Hollweg, J. V. 1999, JGR, 104, 14811
 Hollweg, J. V. & Markovskii, S. A. 2002, JGR, 107, 1080
 Hollweg, J. V., Verscharen, D. & Chandran, D. G. 2014, ApJ, 788, 35
 Howes, G. G., Cowley, S. C., Dorland, W., et al. 2008, JGR, 113, A05103
 Howes, G. G., & Quataert, E. 2010, ApJL, 709, 49
 Howes, G. G., Bale, S. D., Klein, K. G., et al. 2012, ApJL, 753, 19
 Huang, S. Y., Zhou, M., Sahradi, F., et al. 2012, GeoRL, 39, L11104
 Hunana, P., Goldstein, M. L., Passot, T. et al. 2013, ApJ, 766, 93

- Kennel, C. F. & Wong, H. V. 1967, *JPIPh*, 1, 75
- Kellog, P. J., & Horbury, T. S. 2005, *AnGeo.*, 23,, 3765
- Klein, K. G., Howes, G. G., TenBarge, J. M., et al. 2012, *ApJ*, 755, 159
- Krauss-Varban, D., Omidi, N., & Quest, K. B. 1994, *JGR*, 99, 5987
- Lysak, R. L., & Lotko, W. 1996, *JGR*, 101, 5058
- Marsch, E. 2006, *LRSP*, 3, 1
- Podesta, J. J., & Gary, S. P. 2011, *ApJ*, 734, 15
- Podesta, J. J., & TenBarge, J. M. 2012, *JGR*, 117, A10106
- Podesta, J. J. 2013, *SoPh*, 286, 529
- Roberts, O. W., Li, X., & Li, B. 2013, *ApJ*, 769, 58
- Sahraoui, F., Goldstein, M. L., Robert, P., & Khotyaintsev, Yu. V. 2009, *PhRL*, 102, 231102
- Sahraoui, F., Goldstein, M. L., Belmont, G., Canu, P., & Rezeau, L. 2010, *PhRL*, 105, 131101
- Sahraoui, F., Belmont, G., & Goldstein, M. L. 2012, *ApJ*, 748, 100
- Schekochihin, A. A., Cowley, S. C., Dorland, W., et al. 2009, *ApJS*, 182, 310
- Shukla, P. K., & Stenflo, L. 2000, *JPIPh*. 64, 125
- Stasiewicz, K., Bellan, P., Chaston, C. et al. 2000, *SSRv*, 92, 423
- Stringer, T. E. 1963, *JNuE*. 5, 89
- Voitenko, Y., & Goossens, M. 2002, *SoPh*, 206, 285
- Voitenko, Y., & Goossens, M. 2003, *SSRv*, 107, 387
- Voitenko, Y., & Goossens, M. 2006, *SSRv*, 122, 255
- Yao, S., He, J.-S., Marsch, E., et al. 2011, *ApJ*, 728, 146
- Yao, S., He, J.-S., Tu, C.-Y., & Marsch, E. 2013, *ApJ*, 774, 59
- Zhao, J. S., Wu, D. J., & Lu, J. Y. 2010, *JGR*, 115, 12227
- Zhao, J. S., Wu, D. J., & Lu, J. Y. 2011, *ApJ*, 735, 114
- Zhao, J. S., Wu, D. J., & Lu, J. Y. 2013, *ApJ*, 767, 109
- Zhao, J. S., Voitenko, Y., Wu, D. J., & De Keyser, J. 2014, *ApJ*, 785, 139